ARTICLE IN PRESS

Quaternary International xxx (xxxx) xxx

Contents lists available at ScienceDirect

Quaternary International

journal homepage: www.elsevier.com/locate/quaint

Projected climate change impacts in the Tahoe Basin: Recent findings from global climate models

Robert Coats[a,*], Jack Lewis[b], Geoffrey Schladow[c]

[a] Tahoe Environmental Research Center, One Shields Ave., University of California at Davis, Davis, CA, 95616, USA
[b] USDA Forest Service (Ret.), P.O. Box 896, Blue Lake, CA, 95525, USA
[c] Tahoe Environmental Research Center, University of California, One Shields Ave., University of California at Davis, Davis, CA, 95616, USA

ARTICLE INFO

Keywords:
Tahoe
Climate change
Climate models
Precipitation
Temperature
Floods

ABSTRACT

Since 2002, the Tahoe Environmental Research Center has been studying the effects of climate change in the Tahoe Basin. We are using the output from four General Circulation Models downscaled by the method of Localized Constructed Analogues and provided by the Scripps Institution of Oceanography (SIO). The daily data were used by SIO to drive the Variable Infiltration Capacity (VIC) model and derive a suite of 24 hydrologic and climate variables at a 1/16° (*ca.* 6 km) grid scale, for two Representative Concentration Pathways (RCP 4.5 and 8.5). Here we focus on trends in the return levels of extreme climatic events, including annual maximum daily discharge of six basin streams, maximum and total annual kinetic energy (KE) of raindrops falling on snow-free ground, basin-wide climatic water deficit, and wind speed. To analyze time trends in historic and modeled future extreme values, we applied the program extRemes, based on the Generalized Extreme Value (GEV) distribution.

Values of KE on snow-free ground were derived by statistically disaggregating daily rainfall to hourly, and using literature values to convert rainfall intensity (mm/hr) for days without snowpack to KE (Joules/m^2/hr). We found strong upward trends in extreme values, with most of the effect due to loss of snowpack, but a significant effect of increasing rainfall for one model. To estimate future trends in maximum annual daily discharge of six streams, we adjusted the modeled future annual maximum runoff to the distribution of gage data, using regression of gage data on modeled historic runoff at equal return intervals. The GEV results for the six streams, averaged across the four models, indicate an increase in the 20-year flood of 65–117 percent. Climatic water deficit showed strong upward trends for three of the four models, with a maximum at mid-century for one model. Averaged across the basin and across the four models, average and maximum seasonal winds under RCP 8.5 are projected to decrease slightly in all seasons. The trends in averages and extreme values that we found will have important effects on vegetation, wildfire severity, flood hazards and the clarity of Lake Tahoe.

1. Introduction

Lake Tahoe is a large ultra-oligotrophic lake lying at an elevation of 1898 m in the central Sierra Nevada on the California-Nevada border. The lake is renowned for its deep cobalt-blue color and clarity. Due to concerns about progressive eutrophication and loss of clarity, the lake has been studied intensively since the mid-1960s, and has been the focus of major efforts to halt the trends in clarity and trophic status (Goldman 1981, 1988; TERC, 2020).

The long-term trends in lake clarity and water quality are strongly influenced by climate change. Previous work on the effects of climate change on the Tahoe basin watershed showed 1) strong upward trends in air temperature, especially at night; 2) a shift from snowfall to rain; 3) a shift toward earlier snowmelt; 4) increased rainfall intensity and inter-annual variability; 5) increased risk of flooding in the Upper Truckee River basin; 6) increased drought severity, especially in the late 21st century (Coats, 2010; Coats et al., 2013). Work on the Lake itself has shown that 1) the lake is warming at an average rate of about 0.013 °C yr^{-1}; 2) the warming trend in the lake is driven primarily by increasing air temperature, and secondarily by increased downward long-wave radiation; 3) the warming of the lake is modifying its thermal structure, increasing its resistance to deep mixing and threatening the periodic ventilation of the hypolimnion (Coats et al., 2006; Sahoo et al., 2013).

* Corresponding author.
E-mail addresses: RNCoats@UCDavis.edu (R. Coats), jacklewis@suddenlink.net (J. Lewis), gschladow@ucdavis.edu (G. Schladow).

https://doi.org/10.1016/j.quaint.2021.01.006
Received 4 June 2019; Received in revised form 23 December 2020; Accepted 5 January 2021
Available online 5 February 2021

Please cite this article as: Robert Coats, *Quaternary International*, https://doi.org/10.1016/j.quaint.2021.01.006

Recent work at the Southwest Climate Science Center (SWCSC) of Scripps Institution of Oceanography has provided output from a suite of General Circulation Models (GCM's) downscaled to a 1/16° (*ca.* 6 km) grid scale and used to drive the Variable Infiltration Capacity (VIC) model, which in turn produced daily values for historic (1950–2005) and future (2006–2100) periods under two greenhouse gas concentration pathways. The purpose of this study is to use this data set for the Tahoe basin to examine long-term projected trends in annual averages and extreme values of hydroclimatic variables that will have important ecological, water quality and geomorphic impacts. These variables include maximum (Tmax) and minimum (Tmin) daily temperature, precipitation, total and annual maximum hourly rainfall kinetic energy on snow-free ground, climatic water deficit, annual maximum daily stream discharge, and seasonal average and maximum wind speed.

Patterns and trends of precipitation and temperature in the Tahoe basin reflect the patterns and trends in the global climate system, including the position and stability of the jet stream. Francis and Vavrus (2015) analyzed the factors affecting the behavior of the jet stream, and found evidence that rapid warming of the arctic is increasing the amplitude of jet stream meanders and slowing the eastward progression of peaks and troughs, and thus contributing to persistent weather patterns and extreme events in temperate regions.

In Western North America, the interannual variability of temperature and precipitation are strongly influenced by large-scale modes of variability in sea surface temperature (SST) and atmospheric pressure. Two of the most important of these are the Pacific Decadal Oscillation (PDO) and the El Niño-Southern Oscillation (ENSO). The warm (positive) phase of the PDO is characterized by above average SSTs in the eastern North Pacific, and below average SSTs in the central and western North Pacific. The oscillation occurs over time periods of 10–40 years (Mantua et al., 1997). The onset of a strong warming trend at Tahoe coincided with a shift to a positive PDO in about 1976–77. The warm phase of the ENSO (El Niño) involves an eastward flow of warm surface water from the tropical western Pacific toward the west coasts of North and South America. The warmer water and atmospheric pressure distribution affect the storm tracks on the west coast, producing drier winters in the Pacific Northwest, and wetter winters in the Southwest. The cool phase—La Niña —has the opposite effect (Cayan et al., 2016). The Tahoe basin lies near the boundary between the Northwest and Southwest regions, so the ENSO is not a reliable predictor of the Basin's winter precipitation. Analysis of 14 long-term precipitation records in California shows that annual precipitation is decreasing in the south and increasing in the north, trends that may be linked to the behavior of the PDO and ENSO (Killam et al., 2014).

The recent (and apparently on-going) severe drought in southwestern North America (2000–2018) was the second-driest 19-year period since 800 CE, exceeded only by the late 1500s megadrought (Williams et al., 2020). The immediate cause of the drought is a persistent ridge of high pressure in the North Pacific that diverts storms away from California and into the Pacific Northwest. Recent modeling work found evidence that this "ridiculously resilient ridge" (as it is popularly known) is linked to the rapid loss of Arctic sea ice and its impact on convection changes in the tropical Pacific. Continued melting of Arctic sea-ice may be expected to result in a 10–15% decrease in the long-term average annual precipitation in California (Cvjanovic et al., 2017) as well as extreme precipitation in California, through its influence on the transport of heat and vapor from the Arctic Ocean to the Central Pacific (Kennel and Yulaeva 2020). Using tree-ring reconstructions and a suite of 31 climate models, Williams et al. (2020) found that anthropogenic trends in temperature, relative humidity and precipitation account for an average of 47 percent of the severity of the current megadrought.

In the Tahoe region (and much of the U.S. west coast), the majority of precipitation extremes occur in association with winter-time atmospheric rivers (ARs) – long conduits of water vapor transport extending from the tropics that result in high winds and heavy orographic precipitation when they make landfall (Zhu and Newell 1994; Dettinger 2011; Dettinger et al., 2011). Due to the tropical origins of many of these storms, they tend to be relatively warm and cause high runoff volumes, since rapid snowmelt coincides with heavy rainfall (Neiman et al., 2008).

AR storms are now rated on a scale of 1–5 based on their duration and intensity of vapor transport (Ralph et al., 2019). The flood damage from AR storms increases exponentially with intensity, and with a warmer Pacific Ocean, they will become more intense as they become wetter, longer and wider (Corringham et al., 2019; Huang et al., 2020). Gao et al. (2015) suggest that the amount of AR-induced extreme precipitation along the California coast has the potential to more than double by the end of century.

2. Methods and study area

2.1. The Tahoe Basin

Table 1 summarizes some basic facts about the Lake. Most of the precipitation in the basin falls as snow between November and April, although rainstorms combined with rapid snowmelt account for the highest flows and occasional floods. There is a pronounced annual runoff of snowmelt in late spring and early summer, the timing of which varies from year to year and by location in the basin. In some years, summertime monsoonal storms from the Great Basin bring intense rainfall, especially to high elevations on the east side of the basin.

Fig. 1 shows the distribution of mean annual precipitation across the basin for the period 1981–2010, from the PRISM model (Daly et al., 1994). The rain-shadow effect of the Sierra Crest is clear. In recent years, the climate in northern California has been characterized by multi-year droughts (e.g. 1975–77) punctuated by occasional years of high to extreme precipitation (e.g. 1982–83). In the Tahoe basin, this pattern began to emerge in the mid-1970s (Coats 2010). Fig. ESM-2.2-3 shows the annual precipitation at Tahoe City, 1910–2017, and Table ESM-2.2-3 shows annual average monthly weather data for the same station.

Vegetation in the Lake Tahoe Basin is dominated by a mixed conifer forest of Jeffrey pine (*P. Jeffreyi.)*, lodgepole pine (*P. murrayana*), white fir (*Abies concolor*), and red fir (*A. magnifica*). The basin also contains significant areas of wet meadows and riparian areas, dry meadows, brush fields (with *Arctostaphylos* sp. and *Ceanothus* sp.) and rock outcrop areas, especially at higher elevations. *Ceanothus* is capable of fixing nitrogen, but mountain alder (*Alnus incana* ssp. *tenuifolia*), which grows along many of the basin's streams, springs and seeps, fixes far greater quantities, and contributes measurably to nitrate-N concentrations in small streams (Fleschner et al., 1976; Leonard et al., 1979).

Soils of the Basin are derived primarily from andesitic volcanic rocks and granodiorite, with minor areas of metamorphic rock. Some of the valley bottoms and lower hillslopes are mantled with glacial moraines, or glacial outwash material derived from the parent rock. Cryopsamments, Cryumbrepts, rockland, rock outcrops and rubble and stony colluvium account for over 70 percent of the land area in the basin. The

Table 1
Basic facts about Lake Tahoe.

➢ Volume	156 km^3
➢ Surface Area	498 km^2
➢ Average Depth	313 m
➢ Max. Depth	505 m
➢ Area with depth >10 m	*ca.* 90%
➢ Basin Area	1310 km^2
➢ Elevation	1898 m
➢ Mean Water Res. Time	650 yr
➢ Mean Outflow	2×10^8 m^3
➢ Rate of decline in Secchi Depth ca	25 cm yr^{-1}
➢ Mixing freq. below 450 m about	2 yrs in 7
➢ Well-oxygenated to bottom	

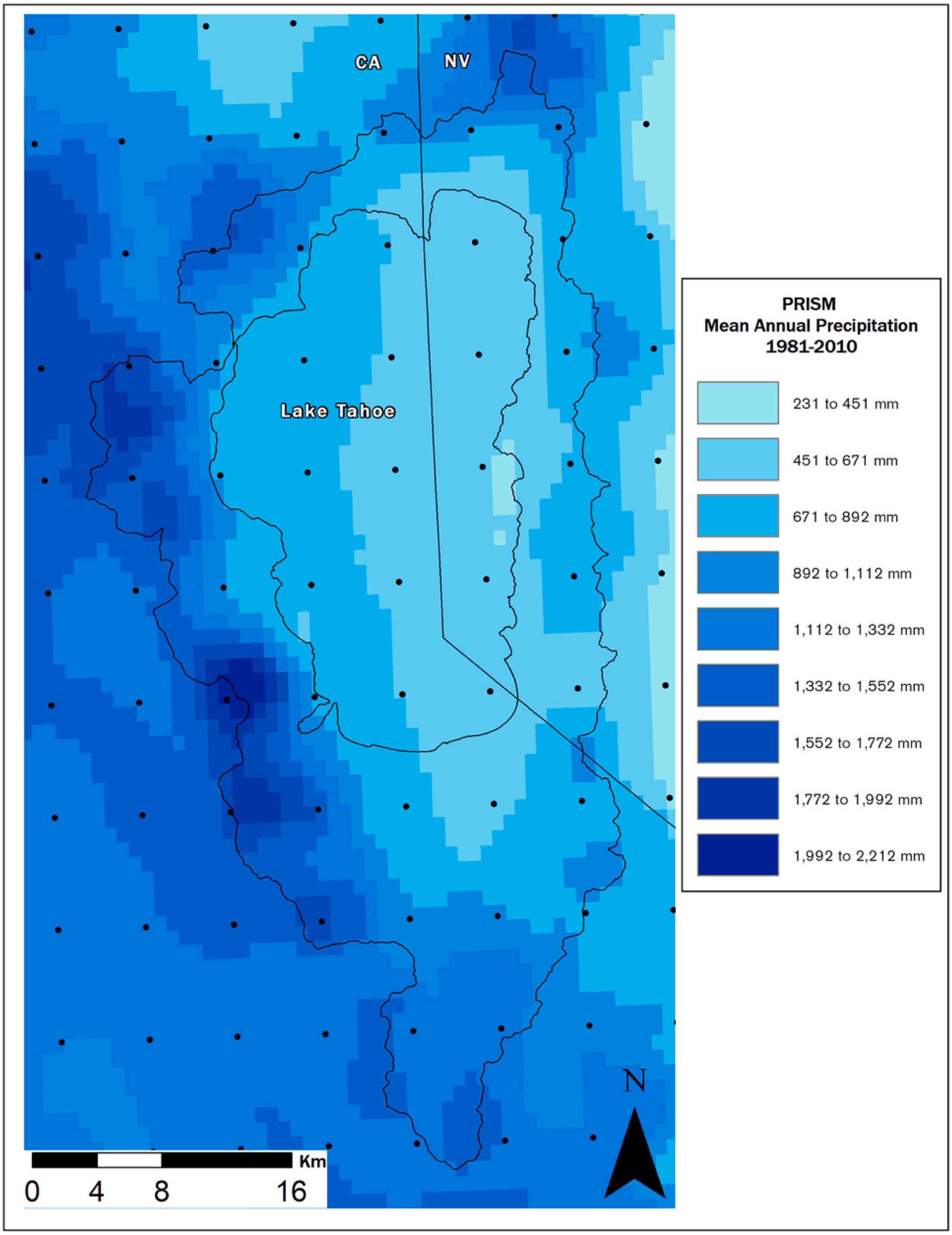

Fig. 1. Average annual precipitation (mm), from PRISM, 1981–2010. Dots indicate the centers of grid cells used in the model downscaling.

basin soils (in the <2 mm fraction) are generally 65–85 percent sand (0.05–2.0 mm) (Loftis, 2007).

Substantial areas of the Basin have been developed for residential and commercial uses, especially along the north, south and west shores. The rate of development was especially intense during the 1960s and 1970s, but has since slowed somewhat due to land use controls.

2.2. Data sources and analysis

For this study, four GCMs (HadGEM2-ES, CNRM-CM5, CanESM2 and MIROC5) and two greenhouse gas trajectories (RCP 4.5 and RCP 8.5) were selected by the Southwest Climate Adaptation Science Center (SW CASC) to cover a range of temperature and moisture trends for the Tahoe basin (Pierce et al., 2018; see Table ESM 2.2–2). The GCMs used are from the Coupled Model Intercomparison Project Vers. 5 (CMIP-5).

These models were also found to be the best of four models from a suite of 20 candidates in terms of their skill in modeling historic precipitation for the period 1980–2005 at a global scale (Lee and Wang 2014). The numbers (4.5 and 8.5) represent different levels of radiative forcing calculated in Watts/m^2 at the top of the troposphere (Van Vuuren et al., 2011; Thomson et al., 2011; Riahi et al., 2011). The radiative forcing is directly related to atmospheric concentrations of greenhouse gasses. Since the RCP 4.5 pathway now seems wildly optimistic, some of the results from that scenario are relegated to the Electronic Supplementary Material.

Using the method of Localized Constructed Analogues (LOCA)

(Pierce et al., 2014), the daily precipitation, temperature (Tmax and Tmin), and wind data were downscaled for us by SW CASC to a 1/16th degree *(ca.* 6 km) grid for the Tahoe Basin (all or part of 50 grid cells), and adjusted using a frequency-dependent bias correction (Pierce et al., 2015). SW CASC then used the corrected LOCA data as input to the Variable Infiltration Capacity (VIC) model (Liang and Lettenmaier, 1994; Hamman et al., 2018; Pierce et al., 2018), producing a suite of 23 hydrologic and meteorological variables, including daily precipitation, daily rainfall, average daily temperature, potential and actual evapotranspiration, runoff and snow water equivalent (SWE) of the snowpack, if any. A historic time period (1950–2005) was included for each model, and the future (2006–2099) was projected for each model/scenario combination.

The time-trends slopes of derived variables and their significance were determined using the non-parametric Mann-Kendall Trend Test (Helsel and Hirsch 2002; Hirsch and Slack 1984). This test has advantages over Ordinary Least Squares Regression in that it is resistant to outliers and does not assume normality of residuals. The software used discounts the p-value for the occurrence of serial correlation (Multitest Version 5.2; Libiseller and Grimvall 2002; Walhlin and Grimvall 2010). Kendall's Tau (τ) indicates the degree of correlation of a variable with time.

Average daily temperature is available from the VIC model, and daily maximum (Tmax) and minimum (Tmin) temperature are available directly from the LOCA data. We also plotted time trends in Tmax and Tmin for basin-wide four-model ensemble averages, and for the eight model-scenario combinations. We plotted trends in average daily temperature for each of four seasons: winter (JFM), spring (AMJ), summer (JAS) and fall (OND).

For daily precipitation, we plotted trends for the eight model-scenario combinations, and for the basin-wide ensemble average. For the modeled historic period, we compared the percentage of total annual precipitation falling in each season given by each model, with the percentage of total annual precipitation for each season from the Tahoe City gage record.

The difference between potential and actual evapotranspiration (Et) is the Climatic Water Deficit (CWD). These variables are calculated in VIC using a three-layer soil water balance model. VIC uses average daily temperature, solar radiation, relative humidity, wind speed and soil water holding capacity (averaged over each grid cell) as input to the Penman-Montieth equation to calculate daily Potential Et. CWD is thus an integrative variable that is closely related to the ecological impacts of climate change. A trend toward higher annual CWD implies a trend toward increasing drought.

The shift in precipitation from snow to rain and acceleration of snowmelt have been well-documented for the Sierra Nevada (Pierce et al., 2008) These changes portend increased kinetic energy (KE) of rainfall on snow-free ground and acceleration of soil erosion. By working with raindrop KE rather than intensity we can quantify the increase in annual total raindrop energy as well as the annual maximum of hourly rainfall. Hourly data for temperature and precipitation are available from a network of nine SNOTEL gages in or near the Tahoe Basin (Natural Resource Conservation Service, 2017) for the period 2008–2016. Locations of those gages are shown in Fig. ESM-2.2-2 and station names are shown in Table 2.

To eliminate snowfall from KE calculations, we first filtered out precipitation that fell when the hourly temperature was below 0 °C. For each of the 44 cells over land in the basin, we then disaggregated the modeled daily rainfall on snow free ground (i.e. on days when the SWE in the cell was less than 1 mm) to hourly values using the statistical distribution of hourly values from the nearest SNOTEL station (identified using the Near tool in ArcGIS10). For details on the method used to disaggregate the daily precipitation data to hourly, see Electronic Supplementary Information (ESM) Page 12, or Lewis and Coats (2020).

We used literature values of the relationship between hourly intensity and kinetic energy (KE) of raindrops (Sempere-Torres, 1992; Wischmeier and Smith, 1958; McCall, 2013). We fitted the Generalized Extreme Value Distribution Function (GEV df) to the projected annual hourly maximum and annual total KE of rainfall on snow-free ground using the statistical package *extRemes*. For each scenario, we pooled KE results from the 4 GCMs. The GEV df (Coles, 2001) is theoretically justified for fitting to maxima of long blocks of data such as the 365 days in a year. The *extRemes* package (Gilleland, 2016) in R (R Core Team, 2017) implements methods for stationary and non-stationary extreme value analysis including GEV-fitting and allowed us to examine time trends not only in average values, but also trends in the levels at 2, 20 and 100-yr recurrence intervals.

Table 2
General Circulation Models used in this study.

Model name	Organization
CanESM2	Canadian Center for Climate Modeling and Analysis, Victoria, BC, Canada
CNRM-CM5	Center National de Recherches Meteorologiques, Meteo-France, and CERFACS (Center Europeen de Recherches et de Formation Avancee en Calcul Scientifique), Toulouse, France
HadGEM2-ES	Met Office Hadley Center, Exeter, Devon, UK
MIROC5 Kanagawa, Japan	Japan Agency for Marine-Earth Science and Technology,

The VIC model uses the water balance approach to calculate daily runoff, defined as surface flow plus infiltration to soil and groundwater. "Runoff" is not the same thing as streamflow, which is influenced by routing of water in the channel system. The excellent record from the USGS stream gages in the Tahoe Basin, however, presents an opportunity to estimate future flooding, expressed as the annual maximum mean daily discharge (MDQ). Six streams in the Basin have discharge records of >30 years: Ward, Blackwood, General, Trout, Third and the Upper Truckee River (UTR). Fig. 2 shows the locations of these streams.

We estimated long-term trends in the flood frequency relationships for these streams in the following steps:

1) For each of six tributary streams in the basin we found the fraction of each 6-km cell that intersects the area of the stream's watershed, and weighted the modeled daily runoff accordingly, for the historic and projected future conditions.
2) We pooled the historic annual maximum daily (AMD) VIC runoff for the four models at each of the six tributaries, 1972–2005, and calculated return levels of annual maximum runoff (cfs) for the 1.01, 2, 5, 10, 25, 50, 100 and 200 year events, using the Log Pearson III method (Helsel and Hirsch 2002).
3) We obtained from the USGS record the mean daily discharge (MDQ) for each tributary gage, 1972–2005 and applied the Log Pearson frequency analysis to the annual maximum series.
4) For each model, we ran regressions of the gage flood levels vs. modeled historic AMD VIC runoff at equal return intervals, and used the derived quadratic equations to adjust the future AMD VIC runoff (for the two emission scenarios) to the gage record distributions. Figs ESM-2.2-4 (a), (b) and c) show the adjustment curves for the 6 streams.
5) We then used the Generalized Extreme Value distribution (GEV) to derive time trends in the magnitudes of the 2, 20 and 100-year discharge events for each of the six streams.

Wind is an important variable that drives mixing of the lake. It also influences evaporation, evapotranspiration, snowmelt and fire behavior, so the seasonal distribution of trends in wind speed may be important. Using the direct-downscaled LOCA wind data modeled at 10 m above the surface, we calculated trends in wind speed for winter, spring, summer and fall, for each of the model/scenario combinations. Daily values were squared before averaging, since shear stress on the surface

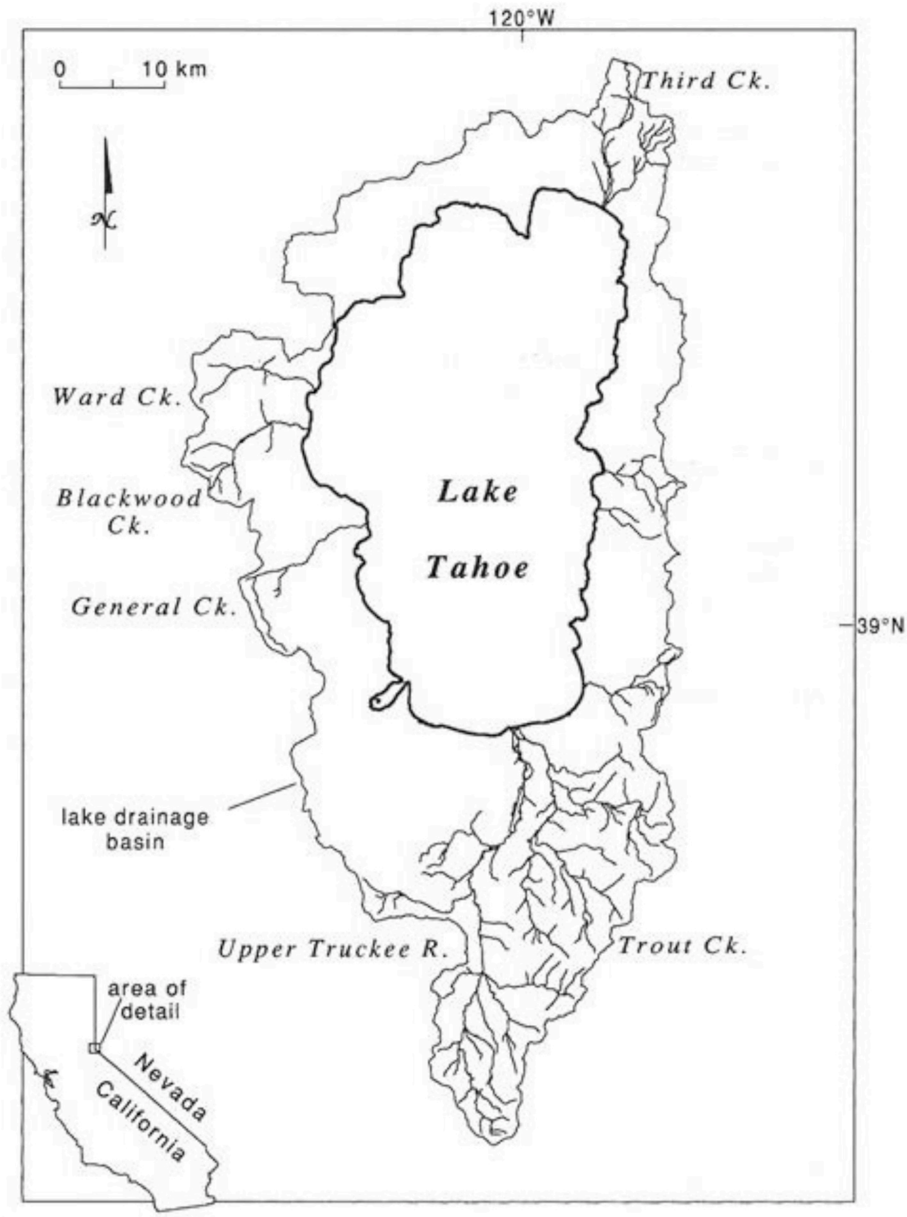

Fig. 2. Map of the Tahoe basin, showing locations of monitored tributary streams.

of the lake, which is important for mixing, is proportional to the square of wind speed.

3. Results

3.1. Temperature

The models, both individually and averaged, project strong upward trends in maximum (Tmax) and minimum (Tmin) daily temperature. Fig. 3 shows the projected future trend together with modeled historic temperature for RCP 8.5. The curves for RCP 4.5 are shown in the Electronic Supplementary Material (ESM-3.1-1). Note that the curves for RCP 8.5 are concave upward, indicating accelerating warming trends. The average slope from 2006 to 2099 is 0.57 °C per decade. The Intergovernmental Panel on Climate Change has warned that "warming of 1.5 °C or higher" above the global mean for pre-industrial levels "increases the risk associated with long-lasting or irreversible changes, such as the loss of some ecosystems." (IPCC, 2018).

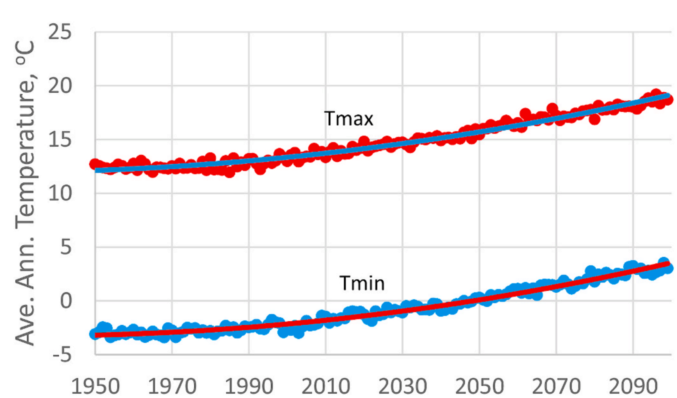

Fig. 3. Basin-wide ensemble average of annual maximum daily (Tmax) and minimum daily temperature (Tmin), for RCP 8.5, with modeled historic temperature.

Fig. 4 shows the warming trends for average daily temperature by season, for the four-model ensemble under RCP 8.5. Trend slopes are shown on the figure. Note that the warmer the season, the faster the change in average temperature, with the highest rate of warming in summer, and the lowest rate in winter. The amplitude of the seasonal temperature variation is thus expected to continue increasing, consistent with the findings of Santer et al. (2018), from satellite and surface data. The rate of change is very consistent across the basin, with little geographic variation detectable in the model output for individual cells. The changes in Tmax and Tmin from the historic (1950–2005) to future (2070–2099) is 5 ± 0.1 °C at all 50 cells. The warming from the historic to end-of-century period is slightly greater (0.14 °C) for Tmax than for Tmin according to a paired *t*-test ($p < 10^{-14}$; $t = 80.3$, d.f. = 49). This lack of geographic variation in warming across the basin most likely reflects the failure of the climate modeling and downscaling to capture the microclimatic effects of topography and the lake.

Air temperature is the most important meteorological variable involved in the warming of Lake Tahoe (Coats et al., 2006 see Fig. ESM-3.1-3). As the lake warms, its thermal stability and resistance to mixing by wind will increase. This is because the relationship between water temperature and density is highly non-linear. For example, the work required to mix layered water masses at 24 and 25 °C is 30 times that required to mix the same masses at 4 and 5 °C (Wetzel, 2001). The deep mixing is responsible for maintaining high dissolved oxygen (DO) levels in the lake's hypolimnion. Under these conditions, the iron in the sediment on the bottom of the lake remains oxidized in the ferric (Fe^{+++}) state, and binds tightly to the phosphorus in the sediment. On average, the 505 m deep lake mixes to the bottom about two years in seven. If the deep mixing and ventilation shut down for a decade or more, the bottom sediments will become anoxic, the ferric iron will be reduced to ferrous (Fe^{++}), and dissolved phosphorus and ammonia will be released to the water column in amounts that far exceed the present loading to the lake from its watershed. When deep mixing finally occurs, fine-grained ferric oxyhydroxide will be released to the water column, algae blooms will become more frequent, and the lake's clarity will be sharply reduced (Beutel and Horne, 2018). The results from a previous modeling study (Sahoo et al., 2013) using output from the Global Fluid Dynamics Laboratory (GFDL) A2 ("business as usual") scenario showed the onset of permanent anoxia at the lake bed by about 2060. The trend in air temperature in that study was only 0.45 °C per decade, so we may expect a somewhat earlier onset of anoxia based on the more recent modeling results reported here.

In the short term however, deep mixing returns the accumulated nutrients, especially nitrogen and phosphorus together with phytoplankton from the hypolimnion of the lake to the photic zone. The algae can survive for several years in the nutrient rich, but totally dark, cold deep waters of the lake (Vincent, 1978; Vincent and Goldman, 1980).

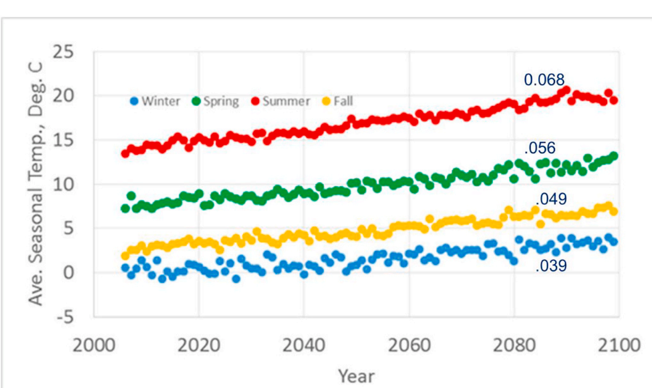

Fig. 4. Average seasonal basin-wide temperature, from four-model ensemble, for RCP 8.5. The linear trend slope in °C/year is shown for each season.

The return of nutrients and associated algal cells to the photic or lighted zone are responsible for the years of highest algal growth and the associated reduced transparency. There is an excellent correlation at Tahoe between the depth of mixing, the annual average algal growth rate and reduced transparency (Jassby et al., 2003).

3.2. Precipitation

The spatial and temporal distribution of precipitation are highly variable throughout the Basin.

Although the ensemble basin-wide average annual precipitation for RCP 8.5 shows a significant upward trend (Fig. ESM-3.2–1), the trend is due entirely to the inclusion of the CanESM2 model, which projects a strong upward trend through the end of this century. None of the other models show this trend, nor does the CanESM2 show it for RCP 4.5.

The four models are, however, very consistent in their partitioning of modeled historic annual precipitation into winter, spring, summer and fall (see Fig. 5(a)). The seasonal partitioning of the four models closely matches that of daily precipitation at the Tahoe City gage for the same period. This is because the modeled precipitation data were adjusted to gridded precipitation data in the bias-correction step.

In Fig. 5, note the shift toward summer precipitation and drier spring and fall according to CansESM2 and (to a lesser extent) in MIROC5. This suggests that CanESM2 is projecting a shift toward a more monsoonal weather pattern compared with historic conditions and the late-century conditions projected by the other three models.

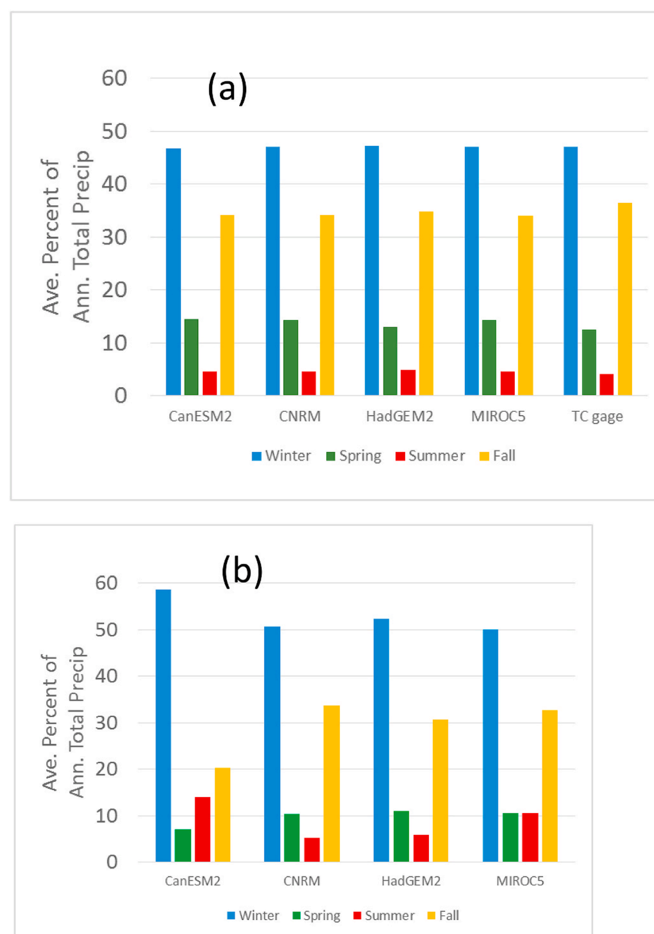

Fig. 5. (a) Seasonal distribution of historic precipitation, 1950–2005, for the four models, compared with distribution for the same period from the gage at Tahoe City.(b) Seasonal distribution of modeled precipitation, 2070–2100, for the four models under RCP 8.5.

A geographic comparison between mean of historical precipitation (1950–2005), and mean of four-model ensemble precipitation, RCP 8.5 (2070–2099), is shown in Fig. ESM-3.2-4. The four-model ensemble for RCP 4.5 precipitation shows that the change over the same time period is only 1–2% across all cells, and is not plotted.

3.3. The future of snow

With air temperatures rising as a result of global warming, a shift from snowfall to rain in the Tahoe basin is inevitable. The moist adiabatic lapse rate is the rate at which the temperature of water-saturated air decreases with elevation. The rate itself varies with temperature, but a typical value is 5.0 °C per km of change in elevation (Minder et al., 2010). The average winter temperature (under RCP 8.5) in the basin is projected to rise about 4 degrees C by 2100, which will raise the elevation of the snow-rain line about 800 m. Thus a storm with the snow level at the lake under current conditions would (on average) produce rain under RCP 8.5 up to an elevation of about 2700 m (about 9000 ft). Fig. ESM 3.3–1 shows the declining fraction of precipitation falling as snow, averaged over the basin, for the four-model ensemble under RCP 8.5. The plot (not shown) for RCP 4.5 also shows a downward trend, but not as steep.

The loss of snowpack in the basin is accelerated not only by the shift from snowfall to rain, but also by the accelerated melting of the pack in the spring thaw. Fig. 6 shows the downward trend in maximum annual Snow Water Equivalent (the depth water stored in the pack) for the modeled future under RCP 8.5 plotted together with the modeled historic snowpack.

3.4. Raindrop kinetic energy on snow-free ground

As the climate warms, the probability of intense rainfall on bare soil will increase 1) since more precipitation will fall as rain rather than snow; 2) the protective snowpack will disappear sooner in the springtime; 3) the frequency of intense high-energy rainfall will increase. Both the maximum hourly and the total annual kinetic energy of rainfall will be affected. These changes will increase the erosion and transport of fine sediment to the lake. Fig. ESM 3.4–1 shows the modeled annual maximum hourly (a,b) and total annual (c,d) raindrop energy on snow-free ground, for the modeled historic period with RCP 4.5 (a,c) and RCP 8.5 (b,d), averaged for the four models over all Tahoe basin cells. Return levels were calculated with the GEV distribution for maximum hourly KE and with the Gaussian distribution for total annual KE.

In order to determine the relative importance of loss of snowpack vs. increased raindrop energy, we detrended the snowpack data for each scenario-model combination, and then repeated GEV analysis. The detrending exercise showed that most of the impact of warming will be due to the loss of snow cover, but increased intensity of rainfall will play a role, especially according to the CanESM2 model results. For details of the KE analysis, see Lewis and Coats (2020).

3.5. Runoff

The VIC model projects modest increases in basin-wide runoff under RCP 8.5 (Fig. ESM 3.5–1), but not under 4.5. These increases are apparently driven by the increase in precipitation, which as noted above, is projected only under the CanESM2 model. The increased precipitation may be offset to some degree by increased evapotranspiration, which is strongly influenced by temperature.

Although the total runoff may not change much as the climate warms the timing of runoff will change dramatically. Fig. 7 shows the shift in monthly runoff from modeled historic conditions to the 2070–2099 period, under RCP 4.5 and RCP 8.5. The month of maximum runoff shifts from June back to May under RCP 4.5, and to January under RCP 8.5, with much lower late summer flow. The shift in runoff is most likely related to the shift from a snowfall to a rainfall regime, with an increase in rain-on-snow events.

3.6. Flood and low flow frequency

Fig. 8 shows the GEV results for time trends in the magnitude of the annual maximum mean daily discharge (MDQ), for the six streams analyzed, with projected floods pooled for the four models, under RCP 8.5. The graphs show, for example, that for the Upper Truckee River (UTR), the current 100-yr event will by the end of the century become a 20-yr event. For Third Creek, the current 100-yr event will become a 20-yr event by about 2060.

The increase in flood frequency has important implications for channel and bank erosion and sediment transport to the lake, as well as for infrastructure, such as roads, culverts and bridges. Using in-channel surveys, numerical modeling and GIS analysis, Simon et al. (2003) found that streambank erosion is an important contributor of suspended sediment from disturbed watersheds, though the contribution of channel materials to fine (<0.062 mm) sediment loads varies widely among the six streams in their study, with the greatest channel contributions (m^3/km/yr, in decreasing order) from the Upper Truckee River, Blackwood, Ward and General Creeks. The trends in flood frequency for these watersheds also suggest that their contributions of fine sediment are likely to increase with climate change, and channels may enlarge to adjust to the increased flood frequency.

The method used here to project future flood frequency-magnitude curves cannot be used to project climate change impacts on low-flow

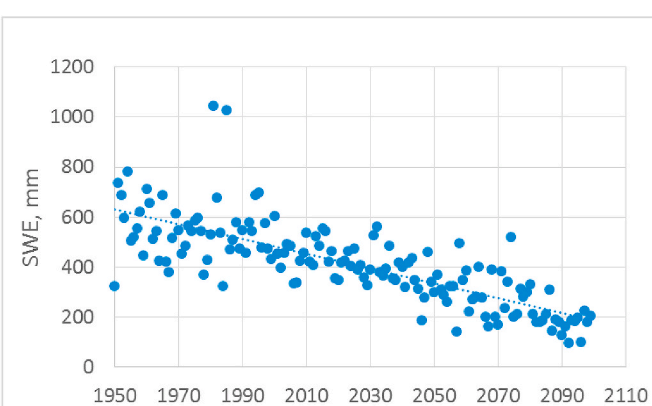

Fig. 6. Trend in maximum annual snowpack (snow water equivalent) in the Tahoe basin, from 4-model ensemble average, for the modeled historic period plotted with modeled future under RCP 8.5.

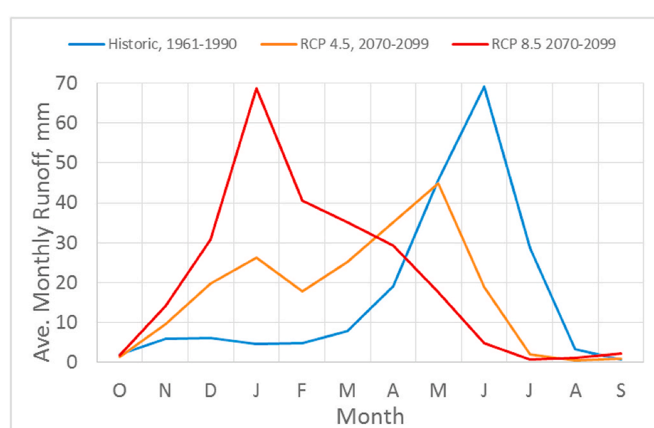

Fig. 7. Timing of monthly runoff in the Tahoe basin, average of four GCMs, for historic and end-of century periods.

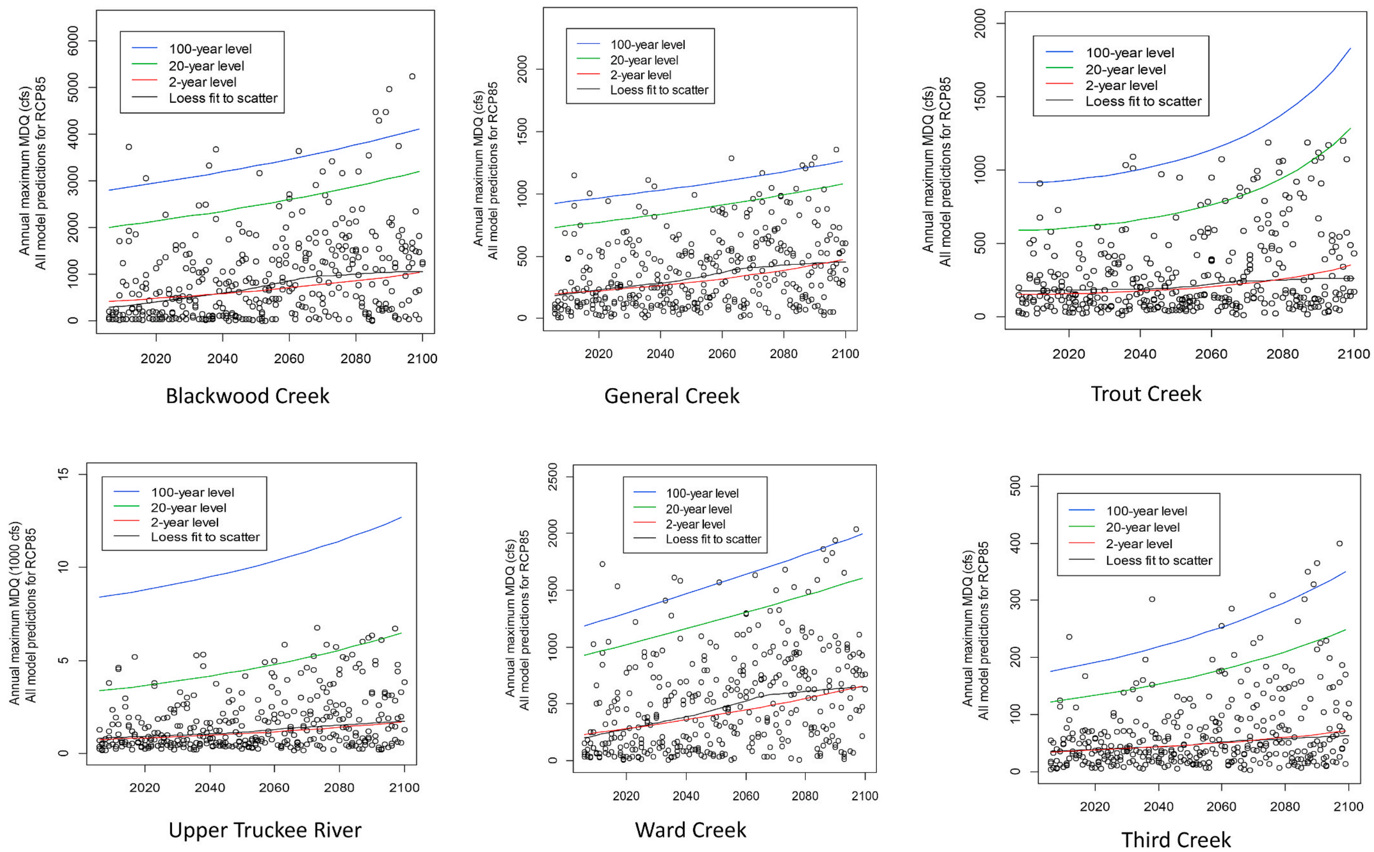

Fig. 8. Trends in annual maximum daily discharge, for the six streams in the Tahoe basin, RCP 8.5, calculated with the Generalized Extreme Values distribution, from pooled model results.

frequency, since during summer, modeled runoff goes to zero, but streams continue to flow. In a previous study, Coats et al. (2013) used daily output from a distributed hydrologic model of the Tahoe Basin (Riverson et al., 2013) to project and bias-correct flow duration curves for the Upper Truckee River (UTR). For a business-as-usual (A2) scenario, the GFDL model projected a downward trend over the 21st century in the minimum annual 5-day low flow of $-0.75\,l\,s^{-1}\,yr^{-1}$ (0.0264 cfs yr^{-1}) ($n = 100$; $p < 0.0073$; $\tau = -0.09$), or a loss of about 27% by 2100. Since our 4-model ensemble projects a higher rate of warming than the GFDL/A2 case, the loss of 27% of the low-flow should be considered a lower limit.

3.7. Climatic water deficit (CWD)

The modeled basin-wide average total annual CWD shows strong upward trends, for both RCP 4.5 and 8.5, with an upward trend slope of 2.0 mm/yr for RCP 8.5 (Fig. 9) and 1.6 mm/yr for RCP 4.5.

The ensemble average however, conceals an important difference among the models. Since the CanESM2 model projects an increase in the precipitation from mid-century onward, the projected CWD with that model reaches a peak in about 2040, and then declines toward the end of the century See Figure ESM 3.7–2.

For three of the GCMs, the VIC hydrologic model projects large and significant increases in the Climatic Water Deficit, exceeding 235 percent (for RCP 8.5) in much of the basin by the end of the century. Fig. 10 shows the change in CWD as percent of the modeled historic conditions. The three-model ensemble projects the most severe increases on the north and east sides of the Basin, where soils are relatively poor, and Available Water Capacity (AWC) is low (Loftis, 2007).

Increasing temperature contributes to the projected rise in CWD in two ways. First, it contributes directly to evapotranspiration. Only with

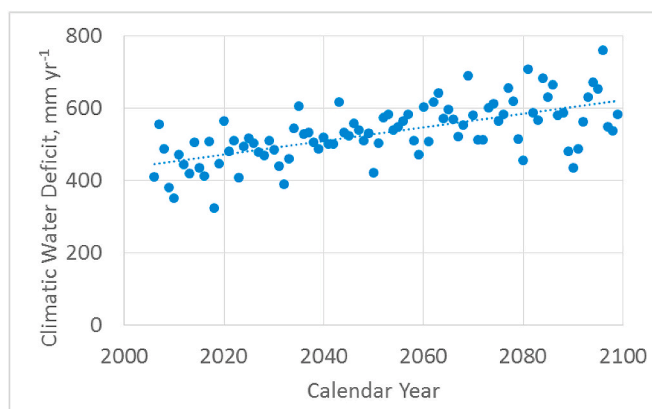

Fig. 9. Modeled future climatic water deficit, annual basin-wide ensemble average, RCP 8.5. Trend slope is 2 mm/yr.

the CANESM2 model is there enough of an increase in late century precipitation to off-set the increase in temperature. Second, the shift from snow to rain, the shift in runoff timing and the loss of the late spring snowpack will result in an earlier on-set of the annual summer drought.

Our projected trend in CWD is consistent with the projected trend in the Palmer Drought Severity Index in the Southwest. Using an empirical drought reconstruction with modeling results from 17 GCMs, Cook et al. (2015) found that "future drought risk will likely exceed even the driest centuries of the Medieval Climate Anomaly … in both moderate (RCP 4.5) and high (RCP 8.5) future emissions scenarios, leading to unprecedented drought conditions …"

The increasing summer drought will have important impacts on the

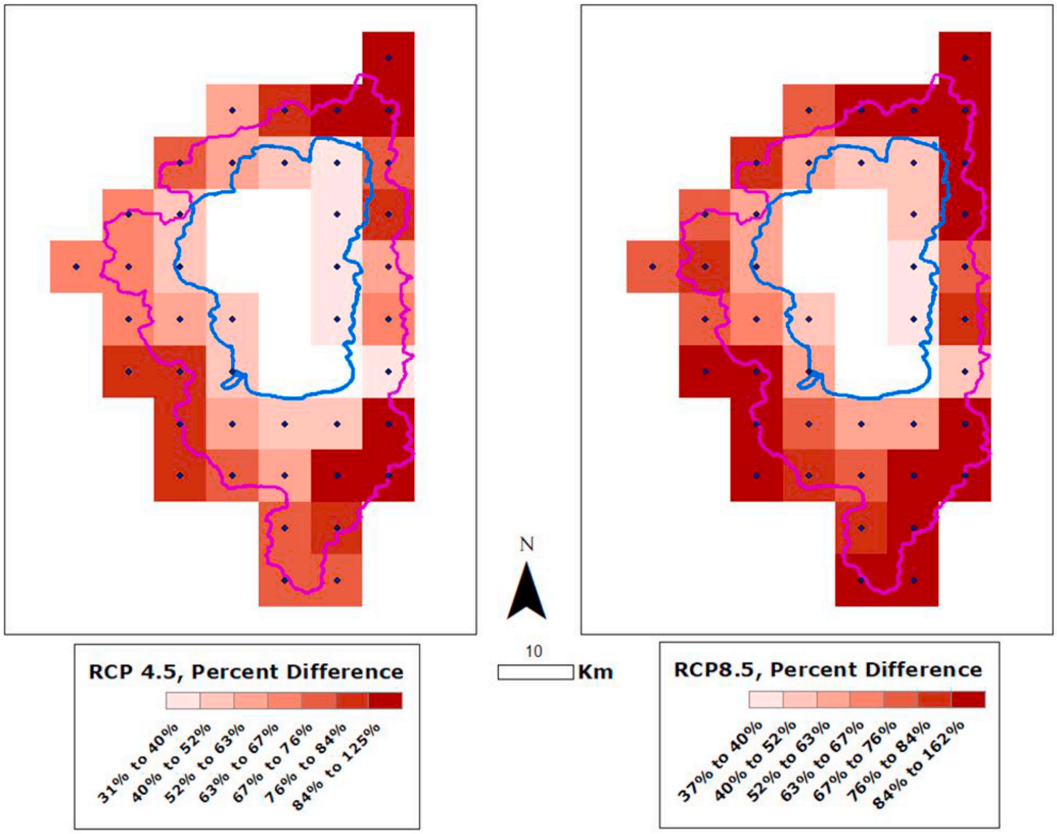

Fig. 10. Percent change in Climatic Water Deficit from the average historic condition (1950–2005) to the average late century (2070–2099) conditions, for the two emission scenarios. The results of CanESM2 are not included, since the late-century summertime moisture in that model differs so markedly from the results for the other three models.

vegetation of the basin. Increasing moisture stress will make the conifer forests more susceptible to bark beetle attack, and lower fuel moisture will increase the frequency and intensity of wildland fire. These changes are already occurring throughout the western US, sometimes with tragic results, and have been widely reported (Westerling et al., 2006; Westerling, 2018). In 2020, wildfires in northern California set new records for the largest fire, and largest area—1700 km^2—burned in a single year, providing grim confirmation of recent predictions by Goss et al. (2020). In the Tahoe basin, two major fires have burned since 2003, with impacts to stream-water quality and the lake itself, though the magnitudes of the water quality impacts depend in part on the location of the fire in relation to the lake and the intensity of rainfall within the first two years after the fire (Oliver et al., 2011).

3.8. Lake warming, wind and deep mixing

If wind speed increases with climate warming, the increase in thermal stability of the lake could be off-set, since the shear stress on the surface of lake is directly related to the square of the wind speed. But the seasonal ensemble averages of the square of daily wind speed show significant downward trends from 2006 to 2100, for all seasons under RCP 8.5 ($n = 96$; $\tau = -0.04$ to -0.09; $p < 0.0004$, by the Mann-Kendall trend test), but show no significant trends under RCP 4.5. See Fig. ESM 3.8–1. It would be useful to examine trends in the square of hourly wind speed, but we do not have hourly wind speed. On a lake as large as Tahoe, however, variation in wind speed at an hourly time scale may by insignificant. Trends in the maximum annual wind speed reflect the downward trends in the annual average.

At Crater Lake, empirical observations and modeling have shown that a decline in spring wind speed as well as increasing spring air temperature over a 25 yr period is associated with the shoaling of stratification depth (Stetler et al., 2020). At Tahoe, however, the magnitude of the changes in both average and maximum spring wind speed are small, and the importance of the downward trends on the lake will have to be analyzed using the Dynamic Lake Model (Sahoo et al., 2013). We can say at this point that there is no projected increase in wind speed to offset the effect of increasing thermal stability of the lake.

3.9. Synergy and uncertainty

As with any complex system, the responses of Tahoe basin ecosystems to climate change will, in many cases, be non-linear, with processes interacting to ameliorate or enhance the impacts of climate change. For example, increasing temperatures will increase the Climatic Water Deficit, and thus increase the moisture stress on vegetation. With rising temperatures and earlier snowmelt at higher elevations, tree growth may be enhanced, and the elevation of the tree line may increase. This would increase the loss of water to evapotranspiration and reduce summer streamflow, as has been shown for the upper Kings River basin in California (Goulden and Bales, 2014). But increased tree cover as the forest cover matures would reduce insolation on the snowpack, and help to maintain early summer streamflow (Winkler et al., 2005).

Effects of climate change on the lake will be similarly complex. Deep mixing of the lake is essential for maintaining DO at the sediment-water interface and keeping biostimulatory phosphorus bound with oxidized iron. But in the short term, occasional deep mixing returns nutrients and dormant phytoplankton to the photic zone, stimulating algae growth and decreasing clarity (Jassby et al., 2003). Fig. 11 is a conceptual model showing some of the complex interactions that influence the effects of climate change on the lake.

Three major sources of uncertainty cast a shadow over this study and similar efforts to project future ecological impacts of climate change.

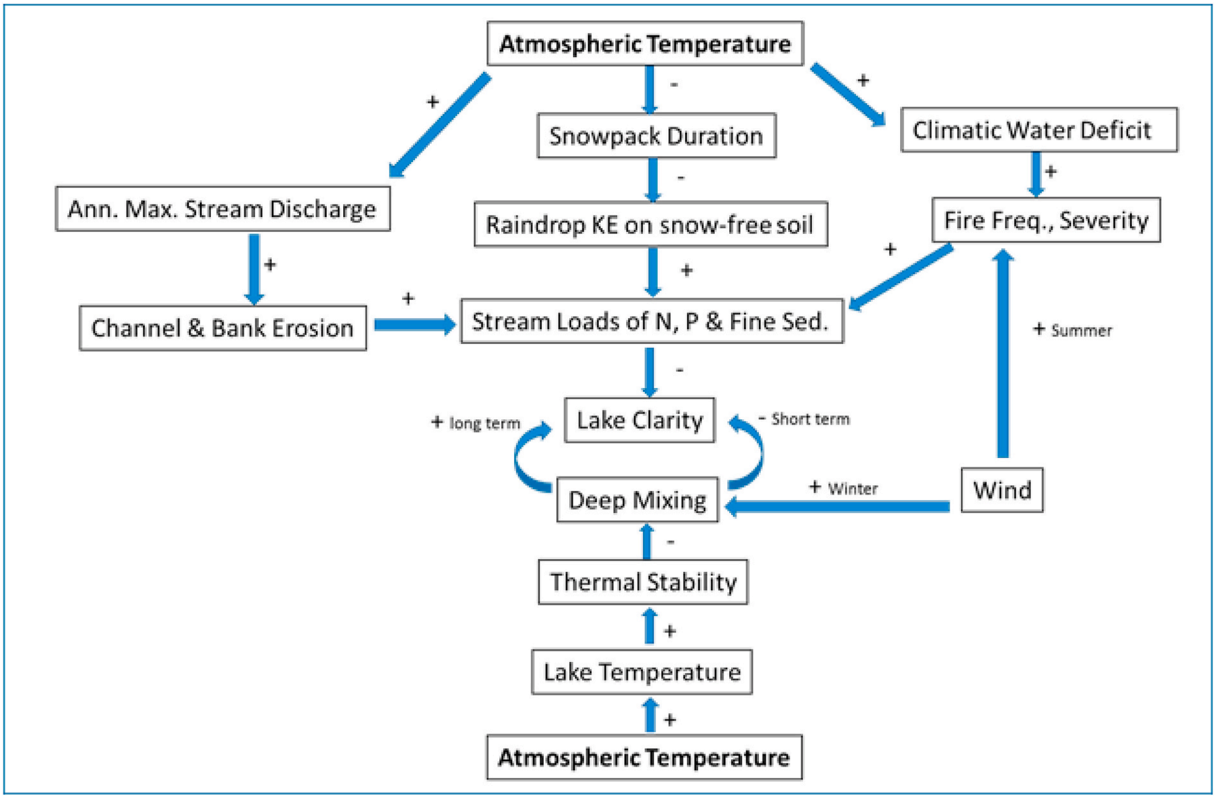

Fig. 11. A Conceptual model showing some of the ways in which climate change may affect Lake Tahoe. Boxes represent ecosystem processes or attributes. Signs next to arrows indicate the direction (positive or negative) of influence.

First, the future trajectory of greenhouse gas (GHG) emissions is essentially unknowable. Alternative scenarios, based on reasonable assumptions about future industrial activity and the success of mitigation efforts, have been developed to take account of this uncertainty, but it must be noted that the actual GHG emissions have in the past exceeded what was thought to be the high-level scenario (Raupach et al., 2007; Manning et al., 2010).

Second, although the models are in good agreement with regard to temperature trends, they do not all agree on the future precipitation for the Tahoe basin. CanESM2 projects a late century increase in annual precipitation with a distinct shift toward wetter summer and drier spring and fall; the other three models do not project a late-century increase. A larger ensemble of models would provide a stronger basis for drawing conclusions based on an average of model results, but with only four models, we can only conclude that a late century increase in precipitation is unlikely, but possible.

A third limitation of the modeling used in this exercise is the relatively course scale. While a 6-km grid is a big improvement over the previously-used 12-km grid, it cannot capture important local climatic effects of topography, vegetation or the lake itself. Development of a regional climate model embedded in or linked to a GCM would be a major step forward.

4. Summary and conclusions

Four GCMs were used with two emissions scenarios to project future climatic changes in the Lake Tahoe Basin. The models are in good agreement on the upward trend in air temperature across the basin, averaging 0.57 °C per decade, for the RCP 8.5 emission scenario. The rate of temperature increase is projected to be highest in summer and lowest in winter. The projected warming will have severe consequences for terrestrial and aquatic ecosystems in the basin.

The four models are in less agreement on the future amount of precipitation in the basin, with three models showing no long-term trend, and one model showing an upward trend. In general, the inter-annual variability in precipitation is increasing, with wet years becoming wetter, and dry years becoming drier. The future climate may be one of prolonged drought punctuated occasionally by years of extreme precipitation and atmospheric rivers.

Increasingly, precipitation will fall as rain rather than snow. The maximum annual snowpack will decrease under all four models, which will increase the kinetic energy of rain drops falling on snow-free ground, and contribute to increased levels of climatic water deficit (CWD). Higher CWD will contribute to greater risk of high-intensity wildfire in the basin.

The shift to earlier dates of melting of the snowpack, together with the shift from snow to rainfall will cause significant increases in the annual maximum of daily discharge, with the current 100-yr event for the Upper Truckee River expected to become a twenty-year event by the end of this century.

Lake Tahoe will continue to warm, and its thermal stability will continue to increase. The lake's increased stability will ultimately shut down the ventilation of the hypolimnion, resulting in releases of bio-stimulatory nitrogen and phosphorus, and fine particles of iron oxy-hydroxide, with concomitant accelerated decline in the lake's clarity.

Data availability

A website will be set up to provide access to the downscaled data from Scripps Institution of Oceanography.

Declaration of competing interest

The authors declare that they have no known competing financial interests or personal relationships that could have appeared to influence the work reported in this paper.

Acknowledgements

We thank David Pierce and Daniel Cayan of the Southwest Climate Adaptation Science Center (SW CASC) at the Scripps Institution of Oceanography for helpful suggestions and providing the down-scaled model output. We thank Zachary Silber-Coats for the geospatial graphics and Goloka Sahoo for downloading the modeled climate data provided by the SW CAS. Funding: Support was provided by the California Energy Commission, the United States Army Corps of Engineers, and the National Oceanic and Atmospheric Administration through the California/Nevada Application Program of the Regional Integrated Sciences and Assessments Program, and by the California Tahoe Conservancy.

Appendix A. Supplementary data

Supplementary data to this article can be found online at https://doi.org/10.1016/j.quaint.2021.01.006.

References

Beutel, M.W., Horne, A.J., 2018. Nutrient fluxes from profundal sediment of ultra-oligotrophic Lake Tahoe, California-Nevada: implications for water quality and management in a changing climate. Water Resour. Res. 54, 1549–1559.

Cayan, D., Dettinger, M., Pierce, D., Das, T., Knowles, N., Ralph, F., Sumargo, E., 2016. Natural variability, anthropogenic climate change, and impacts on water availability and flood extremes in the Western United States. In: Miller, K., Hamlet, A., Kelly, D., Ralph, F., Redmond, K. (Eds.), Water Policy and Planning in a Variable and Changing Climate. Taylor & Francis Group, CRC Press, Boca Raton, FLA, pp. 17–44.

Coats, R., 2010. Climate change in the Tahoe Basin: regional trends, impacts and drivers. Climatic Change. https://doi.org/10.1007/s10584-010-9828-3.

Coats, R., Perez-Losada, J., Schladow, Sg, Richards, R., Goldman, C., 2006. The warming of lake Tahoe. Climatic Change 76, 121–148.

Coats, R., Costa-Cabral, M., Riverson, J., Reuter, J., Sahoo, G., Schladow, G., Wolf, B., 2013. Projected 21st century trends in hydroclimatology of the Tahoe basin. Climatic Change 116, 51–69.

Coles, S., 2001. An Introduction to Statistical Modeling of Extreme Values. Springer-Verlag.

Cook, B.I., Ault, T.R., Smerdon, J.E., 2015. Unprecedented 21st century drought risk in the American southwest and central plains. Sci. Adv. 1, e1400082.

Corringham, T., Ralph, M., Gershunov, A., Cayan, D., Talbot, C., 2019. Atmospheric rivers drive flood damage in the western United States. Sci. Adv. 5, eaax4631.

Cvnjanovic, I., Santer, B., Bonfils, C., Lucas, D., Chang, J., Zimmerman, S., 2017. Future loss of Arctic sea-ice cover could drive a substantial decrease in California's rainfall. Nat. Commun. 8 https://doi.org/10.1038/s41467-017-01907-4.

Daly, C., Neilson, R., Phillips, D., 1994. A statistical-topographic model for mapping climatological precipitation over mountainous terrain. J. Appl. Meteorol. 33, 140–158.

Dettinger, M., 2011. Climate change, atmospheric rivers, and floods in California - a multimodel analysis of storm frequency and magnitude changes. J. Am. Water Resour. Assoc. 47, 514–523.

Dettinger, M., Ralph, F., Das, T., Neiman, P.J., Cayan, D., 2011. Atmospheric rivers, floods and the water resources of California. Water 3, 445–478.

Fleschner, M., Delwiche, C., Goldman, C., 1976. Measuring rates of symbiotic nitrogen nitrogen fixation by *Alnus tenuifolia*. Am. J. Bot. 63, 945–950.

Francis, J., Vavrus, S., 2015. Evidence for a wavier jet stream in response to rapid Arctic warming. Environ. Res. Lett. 10, 014005 https://doi.org/10.1088/1748-9326/10/1/14005.

Gao, Y., Lu, J., Leung, R., Yang, Q., Hagos, S., Qian, Y., 2015. Dynamical and thermodynamical modulations on future changes of landfalling atmospheric rivers over western North America. Geophys. Res. Lett. 42, 7179–7186.

Gilleland, E., 2016. extRemes 2.0: an extreme value analysis package in R. J. Stat. Software 72, 39.

Goldman, C.R., 1981. Lake Tahoe: two decades of change in a nitrogen-deficient oligotrophic lake. Verhandlungen des Internationalen Verein Limnologie 21, 45–70.

Goldman, C., 1988. Primary productivity, nutrients, and transparency during the early onset of eutrophication in ultra-oligotrophic Lake Tahoe, California-Nevada. Limnol. Oceanogr. 33, 1321–1333.

Goss, M., Swain, K., Abatzoglou, J., Sarhadi, A., Kolden, C., Williams, A.P., Diffenbaugh, N., 2020. Climate change is increasing the likelihood of extreme autumn wildfire conditions across California. Environ. Res. Lett. 15, 094016 https://doi.org/10.1088/1748-9326/ab83a7.

Goulden, M.L., Bales, R.C., 2014. Mountain runoff vulnerability to increased evapotranspiration with vegetation expansion. PANAS 111, 14071–14075.

Hamman, J., Nijssen, B., Bohn, T., Gergel, D., Mao, Y., 2018. The Variable Infiltration Capacity model version 5 (VIC-5): infrastructure improvements for new applications and reproducibility. Geosci. Model Dev. 11, 3481–3496. https://doi.org/10.5194/gmd-11-3481-2018.

Helsel, D.R., Hirsch, R.M., 2002. Statistical Methods in Water Resources. Techniques of Water Resources Investigations. U.S.Geological Survey, Washington DC, p. 326.

Hirsch, R.M., Slack, J.R., 1984. A non-parametric trend test for seasonal data with serial dependence. Water Resour. Res. 20, 727–732.

Huang, X., Swain, D.L., Hall, A.D., 2020. Future precipitation increase from very high resolution ensemble downscaling of extreme atmospheric river storms in California. Sci. Adv. 6 eaba1323 15 July 2020.

IPCC 2018. Press Release at: https://www.ipcc.ch/2018/10/08/summary-for-policymakers-of-ipcc-special-report-on-global-warming-of-1-5c-approved-by-governments/.

Jassby, A.D., Reuter, J.E., Goldman, C.R., 2003. Determining long-term water quality change in the presence of climatic variability: lake Tahoe (USA). Can. J. Fish. Aquat. Sci. 60, 1452–1461.

Kennel, C., Yulaeva, E., 2020. Influence of arctic sea-ice variability on Pacific trade winds. Proc. Natl. Acad. Sci. Unit. States Am. https://doi.org/10.1073/panas.1717707117.

Killam, D., Bui, A., LaDochy, S., Ramirez, P., Willis, J., Patzert, W., 2014. California getting wetter to the north, drier to the south: natural variability or climate change? Climate 2 (3), 168–180. https://doi.org/10.3390/cli2030168.

Lee, J.-Y., Wang, B., 2014. Future change in global monsoon in the CMIP5. Clim. Dynam. 42, 101–119.

Leonard, R.L., Kaplan, L.A., Elder, J.F., Coats, R.N., Goldman, C.R., 1979. Nutrient transport in surface runoff from a subalpine watershed, Lake Tahoe Basin, Calif. Ecol. Monogr. 49, 281–310.

Lewis, J., Coats, R., 2020. Trends in raindrop kinetic energy with modeled climate warming in the Lake Tahoe Basin. J. Am. Water Resour. Assoc. 1–14. https://doi.org/10.1111/1752-1688.12834.

Liang, X., Lettenmaier, D., 1994. A simple hydrologically based model of land surface water and energy fluxes for general circulation models. J. Geophys. Res. 99, 14,415-414,428.

Libiseller, C., Grimvall, A., 2002. Performance of partial Mann-Kendall test for trend detection in the presence of covariates. Environmetrics 13, 71–84.

Loftis, W.R., 2007. Soil survey of the Tahoe Basin area, California and Nevada. United States Department of Agriculture, Natural Resources Conservation Service. Accessible online at: http://soils.usda.gov/survey/printed_surveys/.

Manning, M.R., Edmonds, J., Emori, S., Grubler, A., Hibbard, K., Joos, F., Kainuma, M., Keeling, R.F., Kram, T., Manning, A.C., Meinshausen, M., Moss, R., Nakicenovic, N., Riahi, K., Rose, S.K., Smith, S., Swart, R., Van Vuure, D.P., 2010. Misrepresentation of the IPCC CO2 emission scenarios. Lett. Nat. Geosci. 3.

Mantua, N., Hare, S., Zhang, Y., Wallace, J., Francis, R., 1997. A Pacific interdecadal climate oscillation with impacts on salmon production. Bull. Am. Meteorol. Soc. 78, 1069–1079.

McCall, K., 2013. Managing Raindrops in the Lake Tahoe Basin: Projected Increase in Kinetic Energy Impact Around Fallen Leaf Lake as Climate Warms Snowfall into Rain. MS Thesis. Humboldt State University, Arcata, CA, p. 36.

Minder, J., Mote, P., Lundquist, J., 2010. Surface temperature lapse rates over complex terrain: lessons from the Cascade Mountains. J. Geophys. Res. 115, D14122.

Natural Resource, 2017. Natural Resource Conservation Service. https://www.wcc.nrcs.usda.gov/snow/. (Accessed 16 May 2019).

Neiman, P., Ralph, F., Wick, G., Lundquist, J., Dettinger, M., 2008. Meteorological Characteristics and Overland Precipitation Impacts of Atmospheric Rivers Affecting the West Coast of North America Based on Eight Years of SSM/I Satellite Observations, 9, pp. 22–46. https://doi.org/10.1175/2007JHM855.1.

Oliver, A.A., Reuter, J.E., Heyvaert, A.C., Dahlgren, R.A., 2011. Water quality response to the Angora fire, Lake Tahoe, California. Biogeochemistry. https://doi.org/10.1007/s10533-011-9657-0.

Pierce, D.W., Barnett, T.P., Hidalgo, H.G., Das, T., Bonfils, C., Santer, B., Bala, G., Dettinger, M., Cayan, D., Mirin, A., Woo, A.W., Nozaw, T., 2008. Attribution of declining western U.S. snowpack to human effects. J. Clim. 21, 6425–6444.

Pierce, D., Cayan, D., Thrasher, B., 2014. Statistical downscaling using localized constructed Analogs (LOCA). J. Hydrometeorol. 15, 2558–2585.

Pierce, D., Cayan, S., Maurer, E., Abatzoglou, J., Hegewisch, K., 2015. Improved bias correction techniques for hydrologic simulation of climate change. J. Hydrometeorol. 16, 2421–2442.

Pierce, D., Kalansky, J., Cayan, D., 2018. Climate, Drought, and Sea Level Rise Scenarios for California's Fourth Climate Change Assessment, California Energy Commission, p. 78. Publication number: CCCA4-CEC-2018-014.

R Core Team, 2017. R: A Language and Environment for Statistical Computing, 3.4.3. R Foundation for Statistical Computing, Vienna, Austria.

Ralph, F., Rutz, J., Cordeira, M., Dettinger, M., Anderson, M., Reynolds, D., Schick, L., Smallcomb, C., 2019. A scale to characterize the strength and impacts of atmospheric rivers. Bull. Am. Meteorol. Soc. 100, 269–289.

Raupach, M.R., Marland, G., Ciais, P., Lequere, C., Canadell, J.G., Field, C.B., 2007. Global and regional drivers of accelerating CO2 emissions. Proc. Natl. Acad. Sci. Unit. States Am. 104, 10288–10293.

Riahi, K., Rao, S., Krey, V., Cho, C., Chirkov, V., Fischer, G., Kindermann, G., Nakicenovic, N., Rafaj, P., 2011. RCP 8.5—a scenario of comparatively high greenhouse gas emissions. Climatic Change 109, 33–57.

Riverson, J., Coats, R., Costal-Cabral, M., Dettinger, M.D., Reuter, J., Sahoo, G.B., Schladow, S.G., 2013. Modeling the transport of nutrients and sediment loads into Lake Tahoe under projected climatic changes. Climatic Change 116, 35–50.

Sahoo, G.B., Schladow, S.G., Reuter, J.E., Coats, R., Dettinger, M., Riverson, J., Wolfe, B., Costa-Cabra, L.M., 2013. The response of Lake Tahoe to climate change. Climatic Change 116, 71–95.

Santer, B., Po-Chedley, S., Zelinka, M.D., Cvijanovic, I., Bonfils, C., Durack, P.J., Fu, Q., Kiehl, J., Mears, C., Painter, J., Pallotta, G., Solomon, S., Wentz, F.J., Zou, C.-Z., 2018. Human influence on the seasonal cycle of tropospheric temperature. Science 361, 245.

Sempere-Torres, D., 1992. Quantification of soil detachment by raindrop impact: performance of classical formulae of kinetic energy in Mediterranean storms. In: Erosion and Sediment Transport Monitoring Programmes in River Basins. IAHS, Oslo, Norway, pp. 115–124.

Simon, A., Langendoen, E., Bingner, R., Wells, A., Heins, N., Jokay, N., Jaramillo, I., 2003. Draft final Lake Tahoe Basin framework implementation study: sediment loadings and channel erosion. In: USDA Agric. Res. Serv, Channel and Watershed Processes Research Unit. National Sedimentation Laboratory, Oxford, Mississippi.

Stetler, J.T., Girdner, S., Mack, J., Winslow, L.A., Leach, T.H., Rose, K.C., 2020. Atmospheric stilling and warming air temperatures drive long-term changes in lake stratification in a large oligotrophic lake. Limnol. Oceanogr. 2020, 1–11. https://doi.org/10.1002/1no.11684. TERC, 2020.

Thomson, A.M., Calvin, K.V., Smith, S.J., Kyle, G.P., Volke, A., Patel, P., Delgado-Arias, S., Bond-Lamberty, B., Wise, M.A., Clarke, L.E., 2011. RCP4.5: a pathway for stabilization of radiative forcing by 2100. Climatic Change 109, 77–94.

Vincent, W.F., 1978. Survival of aphotic phytoplankton in Lake Tahoe throughout prolonged stratification. Verhandlungen des Internationalen Verein Limnologie 20, 401–406.

Vincent, W., Goldman, Cr, 1980. Evidence for algal heterotrophy in lake Tahoe, California-Nevada. Limnol. Oceanogr. 20, 401–406.

Van Vuuren, D.P., Deetman, S., Elzen, M.G.J.D., Hof, A., Isaac, M., Goldewijk, K.K., Kram, T., Beltran, A.M., Stehfest, E., Vliet, J.V., 2011. Exploring the possibility to keep global mean temperature increase below 2°C. Climatic Change 109, 95–116.

Walhlin, K., Grimvall, A., 2010. Roadmap for assessing regional trends in groundwater quality. Environ. Monit. Assess. 165, 217–231.

Westerling, A.L., 2018. Wildfire Simulations for the Fourth California Climate Assessment: Projecting Changes in Extreme Wildfire Events with a Warming Climate. California's Fourth Climate Change Assessment. California Energy Commission.

Westerling, A.L., Hidalgo, H.G., Cayan, D.R., Swetnam, T.W., 2006. Warming and earlier spring increase western U.S. forest wildfire activity. Science 313, 940–943.

Wetzel, R., 2001. Limnology: Lake and River Ecosystems, third ed. ed. Academic Press, New York.

Williams, A.P., Cook, E.R., Smerdon, J.E., Cook, B.I., Abatzoglou, J.T., Bolles, K., Baek, S. H., Badger, A.M., Livneh, B., 2020. Large contribution from anthropogenic warming to an emerging North American megadrought. Science 368, 314–318.

Winkler, R.D., Spittlehouse, D.L., Golding, D.L., 2005. Measured differences in snow accumulation and melt among clearcut, juvenile, and mature forests in southern British Columbia. Hydrol. Process. 19, 51–62.

Wischmeier, W.H., Smith, D.D., 1958. Rainfall energy and its relationship to soil loss. Trans. Am. Geophys. Union 39, 285–291.

Zhu, Y., Newell, R., 1994. Atmospheric rivers and bombs. Geophys. Res. Lett. 21, 1999–2002.